VOLUME 12 NOMOR 1 JUNE 2025 ISSN 2548 – 611X

JURNAL
BIOTEKNOLOGI & BIOSAINS INDONESIA

Homepage Jurnal: http://ejournal.brin.go.id/JBBI/index

IN-SILICO ANALYSIS OF THE INTERACTION BETWEEN D7 PROTEIN FROM THE SALIVARY GLAND OF *Ae. albopictus* AND Thromboxane A2 FOR DEVELOPING ANTIPLATELET AGENT

Analisis In-Silico Interaksi Protein D7 dari Kelenjar Saliva *Ae. albopictus* Terhadap Tromboksan A2 untuk Pengembangan Agen Antiplatelet

Syubbanul Wathon[1]*, Rike Oktarianti[1], Kartika Senjarini[1], Asmoro Lelono[1]
[1]Biology Department, Faculty of Mathematics and Natural Sciences, University of Jember
Jln. Kalimantan No. 37, Sumbersari, 68121, Jember, East Java, Indonesia
*Email: syubbanulwathon@unej.ac.id

ABSTRACT

The salivary glands of mosquito vector diseases contain various biological components which facilitate blood-feeding into the host's body. These components are mostly protein molecules. Numerous protein molecules in the salivary glands have gained substantial research emphasis to determine their role and function, including those in the salivary glands of Ae. albopictus. D7 protein is the main component in Aedes salivary glands, which aids in inhibiting platelet aggregation by binding to the thromboxane A2 (TxA2) during the blood-feeding. TxA2 is a eicosanoid molecule that stimulates platelet aggregation. The protein's ability to bind TxA2 shows that this protein has potential as a new antiplatelet agent. The examination of the D7 protein in binding TxA2 was performed through an in-silico approach using the molecular docking method. This research included selecting the 3D model of the D7 protein and the TxA2 ligand, preparing the 3D model of the D7 protein, native ligands, and test ligands, targeted molecular docking method, validating the molecular docking, analysis and visualization of the docking results. The molecular docking validation shows an RMSD value of 1.657 Å. The results of molecular docking show an ΔG value of -5.60 kcal/mol, meaning that the D7 protein can bind to the TxA2 ligand stably and spontaneously. The active site of the D7 protein in binding the TxA2 ligand consists of several amino acid residues, namely THR 190, GLU 268, TYR 178, PHE 154, ILE 175, ARG176, VAL 293, TYR 248, and TYR 178. The ability of D7 protein to bind TxA2 as an inducer of platelet aggregation has demonstrated its potential as a novel antiplatelet agent. These results can pave further development of drug discovery in the medical and pharmaceutical fields.

***Keywords**: Antiplatelet, D7 protein, Eicosanoid, Molecular docking, TxA2*

ABSTRAK

Kelenjar saliva nyamuk vektor penyakit mengandung berbagai komponen biologis yang memudahkan *blood-feeding* ke tubuh inang. Komponen biologis kelenjar saliva kebanyakan berupa molekul protein. Berbagai molekul protein kelenjar saliva vektor nyamuk terus dipelajari untuk mengetahui peran dan fungsinya, termasuk komponen protein kelenjar saliva *Ae. albopictus.* Protein D7 merupakan komponen utama kelenjar saliva *Aedes* yang berperan menghambat agregasi platelet dengan mengikat Thromboxane A2 (TxA_2) ketika *blood-feeding*. TxA_2 merupakan molekul *eucosanoid* yang memacu agregasi platelet. Kemampuan protein D7 dalam mengikat TxA menunjukkan protein tersebut berpotensi sebagai agen baru trombolitik. Eksplorasi aktivitas protein D7 dalam mengikat TxA2 dapat diketahui melalui pendekatan studi *in silico* dengan metode *molecular docking.* Metode penelitian ini meliputi pemilihan struktur 3D protein D7 dan ligan TxA_2, preparasi struktur 3D protein D7, ligan natif dan ligan uji, metode

***Received**: 12 October 2024* ***Accepted**: 10 December 2024* ***Published**: 5 May 2025*

targeted molecular docking, validasi metode *Molecular Docking*, dan analisis serta visualisasi hasil *molecular docking.* Validasi *molecular docking* mennunjukkan nilai RMSD 1.657 Å. Hasil *molecular docking* antara protein D7 dengan ligan TxA_2 menunjukkan nilai ΔG sebesar -5.60 kcal/mol. Hal ini menunjukkan bahwa protein D7 dapat berikatan dengan ligan TxA_2 secara stabil dan spontan. Sisi aktif protein D7 dalam mengikat ligan TxA_2 terdiri dari beberapa residu asam amino yaitu THR 190, GLU 268, TYR 178, PHE 154, ILE 175, ARG176, VAL 293, TYR 248 dan TYR 178. Kemampuan protein D7 dari *Ae. albopictus* dalam mengikat TxA_2 sebagai *inducer* agregasi platelet telah menunjukkan potensinya sebagai agen baru trombolitik. Hasil ini menjadi dasar untuk studi lanjut dalam pengembangan *drug discovery* di bidang kedokteran dan farmasi.

Kata kunci: *Antiplatelet, Protein D7, Eikosanoid, Molecular docking, TxA2*

INTRODUCTION

The salivary glands of mosquito vector diseases contain various biological components with different functions (Guerrero et al. 2020). In general, these components function as vasodilators and immunomodulatory factors that influence the host's immune response (Wathon et al. 2022b). The vasodilator plays a role in enlarging the host's blood vessels, making it easier for mosquitoes to suck the host's blood. The immunomodulatory component modulates the immune response in the host (Clinton et al. 2023). These components facilitate the mosquito's blood-feeding on the host and are also indirectly utilized by pathogens carried by the vector to penetrate the host's body (Marín-López et al. 2023). For example, the vector for Dengue Hemorrhagic Fever is the salivary glands of *Ae. albopictus* facilitates the blood feeding and the transmission of the dengue virus into the human body (Gómez-Jeria et al. 2020). Research on the biological components from the salivary glands of disease-vector mosquitoes has become crucial in efforts to control infectious and degenerative diseases in tropical regions.

The salivary glands of *Ae. albopictus* was detected to contain immunogenic protein that aids in blood-feeding (Oktarianti et al. 2021). Several immunogenic protein fractions from the salivary glands of *Ae. albopictus* is known to induce host immune responses (Wathon et al. 2022a). Proteins in the salivary glands of *Ae. albopictus* include Apyrase, Serpin, Adenosine Deaminase, the D7 family, and several other proteins (Wichit et al. 2016). Apyrase inhibits platelet aggregation by hydrolyzing ATP and ADP into AMP (Chowdhury et al. 2021). Serpin acts as a protease inhibitor that inhibits serine protease activity in various hemostatic mechanisms in the host body (Shrivastava et al. 2022). Adenosine deaminase plays an anti-inflammatory role by inhibiting the action of proteases secreted by mast cells (Li et al. 2022). The D7 protein is commonly found in vector saliva, including in mosquitoes of the *Aedes* genus (Conway et al. 2016).

D7 protein belongs to Odorant Binding Proteins and determines the success of the blood feeding to the host body (Alvarenga et al. 2022). D7 protein can bind biogenic amine and eicosanoid produced by the host during the blood-feeding (Jablonka et al. 2019). One type of eicosanoid significant for platelet aggregation is the Thromboxane A2 (TxA2) molecule which triggers thrombus formation in an injured area (Alvarenga and Andersen 2023). The molecule belongs to the eicosanoid group which is a lipid-based chemical signal and plays a role in cell inflammatory responses, vasoconstriction, and platelet aggregation (Szczuko et al. 2021). TxA2 triggers platelet activation by binding to the TxA2 receptor located on the platelet cell membrane (Xiang et al. 2019). The presence of D7 protein during the blood-feeding can bind TxA2 as an eicosanoid component of the host (Martin-Martin et al. 2021). By binding TxA2, D7 proteins inhibit its biological activity, helping mosquitoes feed more efficiently by preventing blood clotting and reducing inflammation at the bite site. This shows that the binding between the D7 protein and TxA2 has antago-

nistic properties toward host body homeostasis. The bond can inhibit platelet aggregation in the injured area due to the blood-feeding (Fontaine et al. 2011). As such, D7 protein can prevent platelet aggregation in the host body. This interaction is significant for understanding vector-host dynamics and developing targeted interventions against vector-borne diseases.

That D7 protein inhibits platelet aggregation shows its potential as a new anti-platelet aggregation agent. Meanwhile, the vectorial capacity of *Ae. albopictus*, which constitutes the main vector for transmitting dengue hemorrhagic fever, remains extensively explored for the components and biological functions of its salivary glands (Ferreira-de-Lima et al. 2020). However, the ability of the D7 protein to bind TxA2 is hardly understood. In response, in-silico studies employing the molecular docking method aid in predicting the interaction and binding of a target protein to the test ligand (Torres et al. 2019). In-silico analysis can provide insights into the binding models and interactions between target proteins and ligands. The results of in-silico analysis are important as they can serve as a basis for further testing of the target protein's activity through in-vitro and in-vivo experiments. Through an in-silico approach, this study aimed to explore how the D7 protein from the salivary glands of *Ae. albopictus* in binding TxA2 which can be developed as a new candidate for antiplatelet agent. These outcomes have the potential to drive further progress in drug discovery within the medical and pharmaceutical sectors.

MATERIALS AND METHODS

The Retrieval of the 3D Structure of Protein and Ligand

The amino acid sequence of the D7 protein was obtained from the UniProt database (https://www.uniprot.org/) with accession number Q5MIW6. 3D structure of protein based on amino acid sequence of the D7 protein from *A. albopictus* was obtained from the SWISS-MODEL database (https://swissmodel.expasy.org/). The quality of the protein model's 3D structure was evaluated using various parameters, including Ramachandran Plots, MolProbity, QMEAN, QMEANDisCo, QMQE, and sequence identity values. The best quality of 3D structure model of D7 protein was downloaded in *.pdb* file format (Bienert et al. 2017). The 3D structure model of D7 protein used in this study with the STML code was 3dye.1 which had a native ligand L-Norepinephrine (LNR). The 3D structure of TxA2 ligand with accession number 5280497 was obtained from the PubChem database (https://pubchem.ncbi.nlm.nih.gov/). The 3D structure of TxA2 was downloaded in *.sdf* file format (Wang et al. 2021).

The Preparation and Optimization of 3D Structure of D7 Protein and LNR Native Ligand

The 3D structure of D7 protein bound to the native ligand was removed from all water molecules and non-functional ligands using Autodock 1.5.7 (Scripps Research Institute). Next, the 3D structure of D7 protein and that of the native LNR ligand were separated, with each 3D structure saved in a different *.pdb* files format.

The 3D structure of D7 protein separated from the native LNR ligand was prepared using Autodock Tools, adding polar hydrogen, checking for missing atoms, and adding Kollman Charge. Then, the 3D structure of D7 protein was generated by equalizing the load and setting the files using AutoDock Tools. The 3D structure of D7 protein was then saved in *.pdbqt* file format (Huey et al. 2012).

The 3D structure of LNR native ligand was prepared by adding Gasteiger charges and performing a non-polar merger. The native ligand was prepared by adding a Gasteiger charge and performing a non-polar merger in that only polar hydrogen was enabled to interact with the target protein residue (Sari et al. 2020). Next, the rotation point was set for the LNR native ligand through a torsion tree to determine the best rotation results for the molecular docking. The prepared ligand structure was saved in *.pdbqt* file format (Huey et al. 2012).

The Validation of Molecular Docking Methods

Validation of the molecular docking method was carried out through a re-docking process between the 3D structure of D7

protein and the native ligand LNR. The re-docking determined the binding location between the D7 protein and the TxA2 ligand through gridding in the grid box area using AutoDock Tools. The grid box, indicating where the ligand attached to the protein, showed number point dimension (x, y, and z), spacing (Angstrom), and center grid box (x, y, and z). The point dimension can define the size of the grid box and ensure it covers the entire binding pocket or desired region. Grid spacing can set the grid resolution and determine how finely the space within the box is divided for energy calculations. The grid box is centered around the specific part of the protein, usually the binding site or any predicted active site. The file was saved in *.txt* file format. Validation of molecular docking parameters is determined by an RMSD (Root Mean Square Deviation) below 2 Angstroms (< 2Å) (Ramírez and Caballero 2018). The RMSD value derived from the conformational alignment between the native ligand from re-docking and its crystallographic conformation.

The Preparation of 3D Structure of TxA2 Ligand

The 3D structure of TxA2 ligand was prepared using Chem 3D 15.1 (Cambridge Soft) to minimize ligand energy through the use of Force Field Molecular Mechanism (MM2). The 3D structure of TxA2 was saved in *.pdb* file format. The file was then prepared further via AutoDock Tools by adding polar hydrogen and Gasteiger charge as well as setting rotation through the same stages as the LNR native ligand preparation. The preparation results were saved in *.pdbqt* file format.

The Molecular Docking between D7 Protein and TxA2 Ligand

The molecular docking between the 3D structure of D7 protein and TxA2 ligand was carried out using AutoDock Tools. The 3D structure of D7 protein previously prepared in *.pdbqt* file format were put into one folder, and AutoGrid4 and AutoDock4 programs were added. The D7 protein was arranged as a macromolecule and the TxA2 as a ligand was used for grid box construction. The next stage was setting the grid box based on the coordinates from the previous re-docking.

The results of grid box settings were saved in *.gpf* file format in the same folder. AutoGrid4 was operated using the Command Prompt (CMD) command based on the grid box. Parameter settings (Docking-Search Parameters-Genetic Algoritm-Accept-Docking-Docking Parameters-Accept) and protein stiffening were carried out to enable AutoDock4. The results were saved in a file in *.dpf* file format. AutoDock4 was run via the Command Prompt command based on the Autogrid result and previously created parameters (Endriyatno and Walid 2022).

Analysis and Visualization of Molecular Docking Results between D7 Protein and TxA2 Ligand

The results of molecular docking between the 3D structure of D7 protein and TxA2 ligand were analyzed using free energy value (ΔG), the type of bond formed, and the amino acid residues in forming the chemical bond. The binding conformation at this stage was visualized using BIOVIA Discovery Studio (Minovski 2021).

RESULTS AND DISCUSSION

The 3D models of D7 Protein of *Ae. albopictus*

This study used an amino acid sequence for the D7 protein of *Ae. albopictus* from the UniProt database with accession number Q5MIW6. The D7 protein of *Ae. albopictus* data was identified as long-form D7 salivary protein D7I2. Composed of 323 amino acid sequences, the D7 protein was obtained from the species *Ae. albopictus* (Asian tiger mosquito) (*Stegomyia albopicta*). The protein code and complete amino acid sequence from the D7 protein of *Ae. albopictus* are shown in Table 1.

Table 1. The amino acid sequence of the D7 protein from *Ae albopictus*

Protein Data of D7 *Ae. albopictus* in *.fasta* File Format
tr|Q5MIW6|Q5MIW6_AEDAL Long form D7 salivary protein D7l2 OS=Aedes albopictus OX=7160 PE=2 SV=1
MNILLVLAVVTISSLALVTAKGPFDPEEMHFIFTRCMEDNLKDGPDRVKTLLK-WKEWVTEPKDDPATHCFAKCVLEMSGLYDAASGKFDASVIEAQHKAYPNSEDKGKVDAFVKAV QALPPTKNDCTAVFRAFGPVHMAHKATSINLFHDNKALTKGIYEKLGKDIRQRKQSYFEF-CENKHYPVGSPKRSDLCKIRQYVVLDDAQFKQHTDCIMKGLRYITKDNILNCDEIKRDFKQVNKDT GALEKVLNTCKAKEPRDVKEKSWHYYKCLVESSVANDFKEAFDYREVRSQNYGY-HLMQKQPYNKPAVQAQVSEVDGKQCPS

The 3D structure of D7 protein model was created through homology modelling on the SWISS-MODEL based on amino acid sequence of D7 protein from *Ae. albopictus*. The 3D structure of D7 protein model was selected with the STML ID code, namely 3dye.1. The 3D structure of protein model was the D7 Protein Crystal Structure of the AED7-norepinephrine complex, and this structure showed a native ligand LNR. Based on its conformation, the 3D structure of protein model represented a monomer consisting of one protein chain (chain A). A decent 3D structure of protein model resulted from the visualization of the D7 protein using the X-ray crystallography with a resolution of 1.75 Å. By contrast, a protein structure of X-ray crystallography results with a resolution below 2.5 Å indicates that accurate visualization is gradually achieved (Ramírez and Caballero 2018). The 3D structure of D7 protein model with ID code 3dye.1 is shown in Figure 1.

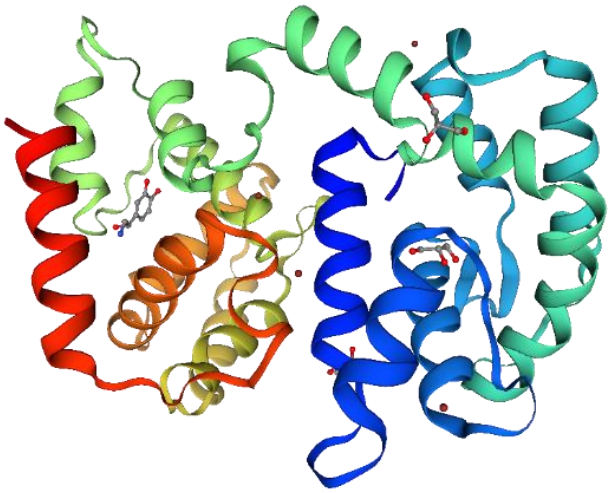

Figure 1. The 3D structure of D7 protein model (STML ID: 3dye.1)

The Assessment of the 3D Structure of D7 Protein Model

The quality of the 3D structure of protein model was assessed through several parameters, namely Ramachandran Plots and MolProbity, QMEAN, QMEANDisCo, QMQE, and Seq Identity values (Ahmed 2021). The 3D structure of protein model was found satisfactory since there were more amino acid residues in the favoured region than those in the outliers region (Sharma et al. 2013). The assessment demonstrated that the 3D structure of D7 protein model had a favoured area of 98.66% and an outliers area of 0.00%. Ramachandran Plots of the 3D structure of D7 protein model are hereby presented in Figure 2.

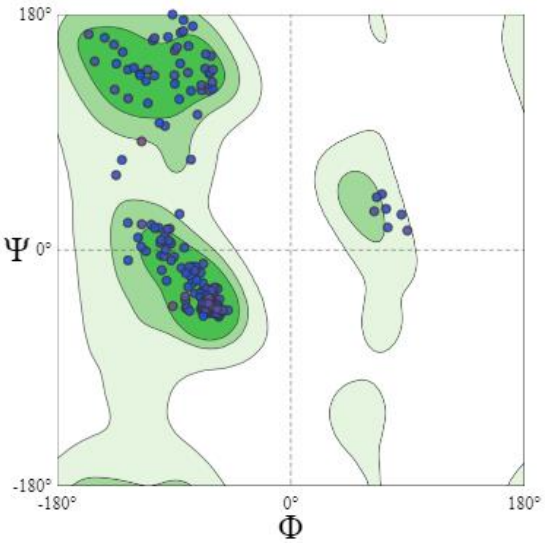

Figure 2. Ramachandran plots of the 3D structure of D7 protein model

Table 2. The analysis of 3D structure of D7 protein model

No.	Parameters	Score
1	MolProbity Score	0,85
2	Clash Score	1,24 (A97 HIS-A104 GLU)
3	Ramachandran favoured	97,99%
4	Ramachandran outliers	0,33% A170 LYS
5	Rotamer Outliers	0,00%
6	C-Beta Deviations	1 A149 HIS
7	Bad Bonds	0/2499
8	Bad Angels	11/3369 A150 ASP, A165 ASP, A97 HIS, (A306 LYS-A307 PRO), A43 ASP, A241 ASP, A266 HIS, A209 HIS, A68 HIS, A140 HIS, A137 HIS, (A100 TYR-A101 PRO), A297 HIS, A149 HIS
9	Cis Prolines	2/15 (A22 GLY-A23 PRO), (A60 GLU-A61 PRO)

As can be appreciated in Table 2, the MolProbility value is 0.85, which signifies a very decent model. The value denotes a log-weighted combination of clash score, percentage of unfavorable Ramachandran, and percentage of bad side-chain rotamers. It also represents one value to describe crystallographic resolution. Any 3D structure of protein model with a MolProbity value lower than the crystallographic resolution value implies that the protein model quality is better than the average structure at that protein resolution (Chen et al. 2010). The crystallographic resolution value of the 3D structure of the D7 protein model is 1.75 Å.

Another parameter to assess the quality of a 3D structure of protein model is the QMEAN (Qualitative Model Energy Analysis) value which requires bioinformatic analysis and computational biology. This is because the QMEAN value indicates the reliability and accuracy of the 3D structure of a protein model (Studer et al. 2020). The QMEAN value lies between 0-1, with a higher value corresponding to a better model. The SWISS-MODEL database showed that QMEAN values were converted into Z-scores for correlating the relationship between what was expected from high-resolution X-ray structures. The Z-score value

for the 3D structure of D7 protein model was indicated by the position of the model (red asterisk) in the Z-score distribution. The data in Figure 3 demonstrates that the red asterisk is located in the 1<|Z-score|<2 areas and close to the |Z-score|<1 area, which infers satisfactory 3D structure of protein model.

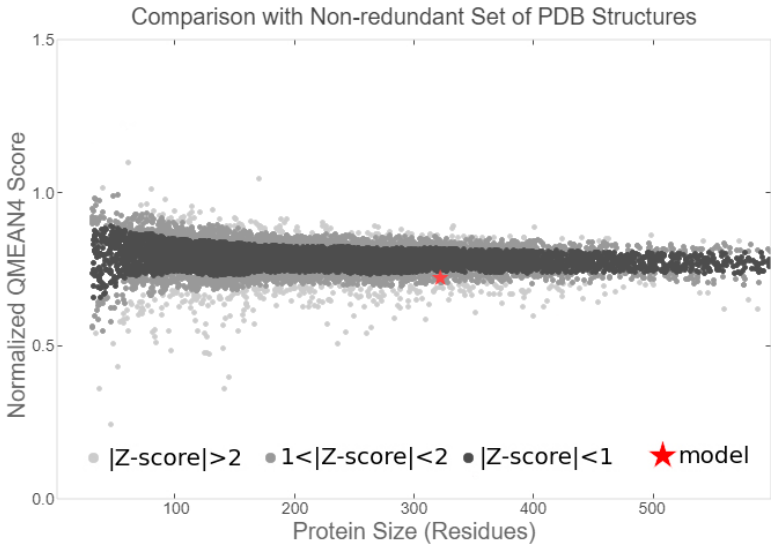

Figure 3. The Z-Score value on the 3D structure of D7 protein model

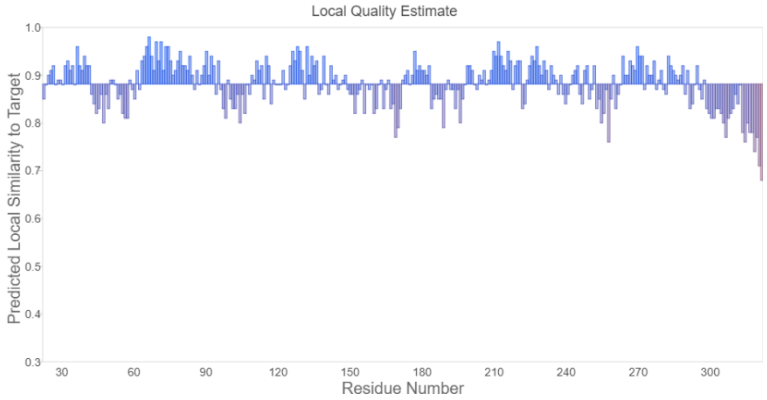

Figure 4. The QMEANDisCo value of the 3D structure of D7 protein model

The QMEANDisCo (Qualitative Model Energy Analysis Distance Constraints) is a combined assessment parameter between global values of the entire protein structure and local values per amino acid residue to determine absolute quality estimates based on one protein model. The QMEANDisCo global value shows the model quality based on the distance constraints of the model protein. The QMEANDisCo global value of 3D model of D7 protein identified in the study was 0.88 ± 0.05. The data in Figure 4 shows the similarity between the model amino acid residues (as the x-axis) and the original structure (y-axis). Based on the local model quality values per amino acid residue, there are no amino acids lower than 0.6. This shows that the amino acid residues of the 3D structure of D7 protein model have good quality. If the QMEANDisCo global value is below 0,6, it indicates signifies poor 3D structure of protein model (Studer et al. 2020).

The GMQE (Global Model Quality Estimate) shows the accuracy rate or match between the 3D structure of a protein model and the corresponding 3D structure of protein model in the SWISS-MODEL database. The GMQE value is expressed as a number from 0 to 1. The GMQE value of the 3D structure of D7 protein model shows a figure of 0.87, which confirms that the 3D structure of protein model has good quality. Any GMQE closer to 1 indicates a higher

accuracy rate of the 3D structure of protein model (Biasini et al. 2014).

The Seq Identity value shows the number of identical residues between the amino acid sequence of a protein and the amino acid sequence of the protein model (Kanduc 2012). The Seq Identity value in the 3D structure of D7 protein model shows 71.19%. The acceptable Seq Identity value is >30%. A higher Seq Identity value indicates the accuracy level between the amino acid sequence and the 3D structure of protein model sequence. If Seq identity value shows <30%, so it is included in the twilight zone, which indicates unsatisfactory accuracy (Khor et al. 2015).

3D Structure of LNR and TxA2 Ligand

The native ligand used in this study came from the 3D structure of the LNR ligand contained in the 3D structure of D7 protein model (3dye.1) obtained from the SWISS-MODEL database (Table 3). Native ligands aided in validating molecular docking and informed test ligands used in the molecular docking. The LNR ligand had the molecular formula C8H11NO3 (Martin-Martin et al. 2020).

Table 3. The 2D and 3D structures of LNR and TxA2 ligand

Ligand Name	Ligand Structure	
	2D Structure	3D Structure
L-Norepinephrine (LNR)	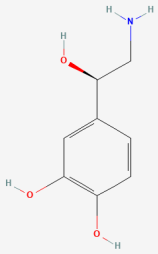	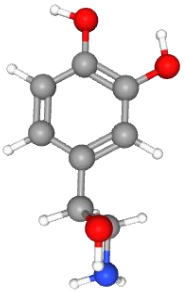
Thromboxane A_2 (TxA2)	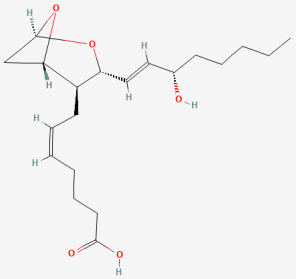	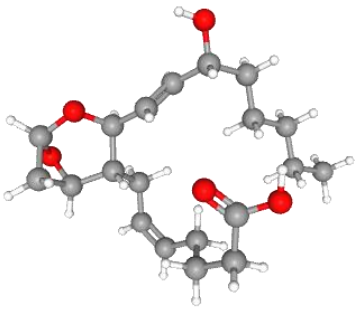

The 3D structure of TxA2 ligand in this study was obtained from the PubChem database with accession number 5280497 (Table 3). The TxA2 compounds is a platelet aggregation agonist produced from platelets and smooth muscle when tissue damage or inflammation occurs in the body by reducing fluid loss in the vascular system (plasma and blood) (Martin-Martin et al. 2020). In addition, the TxA2 has pro-thrombotic properties, stimulating platelet activation and aggregation. The TxA2 is also known to be a vaso-constrictor that is triggered by tissue damage and inflammation. The TxA2 has the molecular formula $C_{20}H_{32}O_5$ (Rucker and Dhamoon 2024).

The Validation of Molecular Docking Methods

The target protein structure was prepared by removing water molecules and non-standard residues to allow the molecular docking (Attique et al. 2019). The native ligand was also separated from the target protein structure to provide binding space or site for the test ligand with the target protein during molecular docking (Susanti et al. 2019). The native ligand of LNR was

separated from the 3D structure of D7 protein. Polar hydrogen atoms were added because the PDB file of the 3D protein structure from X-ray crystallography may not have a hydrogen atom which is essential to make possible binding to the ligand (Ferencz and Lucia 2015). The addition of a hydrogen atom rotated the hydrogen, enabling the ligand and the protein to interact (Sastry et al. 2013). The missing atoms setting aimed to check for missing atoms in the 3D structure of the target protein because the PDB file sometimes contained several missing atoms (Duan et al. 2020). The addition of Kollman charge aimed to add charge, namely electrostatic potential energy, to the amino acids of the target protein (Kolina et al. 2019).

The docking was validated by setting grid box coordinates for the re-docking between the native ligand and the target protein. This was achieved by creating space for the native ligand tethered to the target protein. The resultant space indicated a site for ligands to interact with target proteins (Alhazmi 2015). The grid box settings were determined through the coordinate points on the active site of the target protein, which included the coordinate values of grid size, grid center, and grid spacing (Afriza et al. 2018). The grid box coordinate settings are displayed in Table 4. The LNR native ligand formed a binding conformation with the 3D structure of D7 protein in the grid box.

Table 4. The arrangement of grid box coordinates in the 3D structure of D7 protein

Grid Size	Grid Center	Grid Spacing
x = 40	x = -0.612	
y = 40	y = 0.354	0,375 Å
z = 40	z = 29.11	

The parameter for validating the molecular docking was the RMSD value obtained from conformational alignment between the native ligand resulting from re-docking and the native ligand conformation resulting from crystallography. A smaller RMSD value indicates that the conformation of the re-docked ligand position is closer to the conformation of the original ligand position on the target protein. The RMSD value <2 Å is deemed valid (Ferencz and Lucia 2015). The re-docking showed an RMSD value of 1,130 Å. The overlapping position between the 3D structure of native ligand LNR, the original conformation, and the conformation resulting from the re-docking is shown in Figure 5. The re-docking results show that the molecular docking is acceptable and eligible for further molecular docking between 3D structures of D7 protein and TxA2 test ligands.

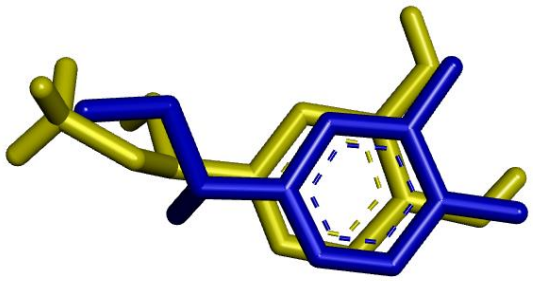

Figure 5. Visualization of the overlaps between the 3D structure of the native ligand LNR, the original crystallographic conformation (blue), and the re-docking conformation (yellow)

The Molecular Docking of D7 protein with TxA2 Ligand

TxA2 ligand was prepared through energy minimization with MM2 settings to obtain a stable 3D conformation. This enabled the ligand to bind to the active site of the target protein (Fadlan and Nusantoro 2021). Likewise, the addition of hydrogen atoms enabled the ligand to bind to the target protein (Sastry et al. 2013). The non-polar

merge arrangement ensured that only polar hydrogen atoms interacted with target protein residues (Sari et al. 2020). Next, ligand preparation went through compute Gasteiger charges settings to add partial charges to the molecule (Alsafi et al. 2020).

The molecular docking involved the D7 protein and TxA2 ligand. The molecular docking was carried out using a grid box arrangement based on the results of re-docking with the native ligand LNR. The grid box coordinate settings were similar to the results of re-docking validation so that the TxA2 ligand bound to the active site of the D7 protein. The 3D structure of D7 protein was rigid while the TxA2 ligand was flexible. This arrangement aimed to ensure that the ligand forms a conformation by binding to the active site of the target protein (Martínez 2015).

The Analysis and Visualization of Molecular Docking Results between D7 Protein and TxA2 Ligand

The molecular docking results between the target protein and the test ligand were evaluated based on the binding energy value, the types of chemical bonds, and the amino acid residues on the active site of the target protein that interact with the ligand (Pratama 2016). The parameter of Gibbs free energy (ΔG) or binding energy is the amount of energy required to form a chemical bond on the active site of D7 protein to the test ligand TxA2. The Gibbs free energy value indicates the bond strength between the target protein and the test ligand (Saputra and Susanti 2018).

The ΔG value resulting from molecular docking between the 3D structure of D7 protein and TxA2 ligand was -5.60 kcal/mol. The substantial ΔG value indicates the amount of energy released when the ligand binds to the target protein, while a smaller ΔG value indicates that lower amount of required energy (Arwansyah et al. 2014). The finding of ΔG value was -5.60 kcal/mol indicates the spontaneous interaction between the protein and the ligand, generally occurring at a constant trend. A ΔG value <0 indicates an irreversible and spontaneous reaction that produces products. The ΔG = 0 indicates a reversible reaction. A ΔG value > 0 indicates that the absence of reaction (Wang et al. 2021). The increasingly negative ΔG value indicates the stronger the bond between the ligand and the target protein (Umamaheswari et al. 2013). In addition, a negative ΔG value indicates that the interaction between molecules occurs exothermically, meaning that the binding between ligands on the active site of a protein is stable and occurs spontaneously (Forouzesh and Mishra 2021). In this study, the D7 protein can bind to the TxA2 molecule stably and spontaneously. These results confirm that during the blood-feeding, D7 protein from *Ae. albopictus* saliva can inhibit platelet aggregation because it can bind and inhibit TxA2.

Previous studies have shown that the D7 protein from the salivary glands of *Ae. albopictus* exhibits binding affinity and interactions with several molecules as ligands. The D7 protein has moderate and stable binding affinity toward histamine. It also exhibits high and stable affinity for dopamine. Furthermore, the D7 protein demonstrates the higher and more stable binding affinity toward norepinephrine. The highest binding affinity and most stable interaction are observed when the D7 protein binds to serotonin. Meanwhile, the D7 protein shows moderate and stable binding affinity for histamine. The D7 protein also has a low but relatively stable binding affinity toward tryptamine. Low binding affinity and unstable interactions are shown by the D7 protein when binding to epinephrine (Martin-Martin et al. 2020).

Another study showed that the D7 protein from the salivary glands of *Ae. aegypti* species exhibits relatively stable binding affinity and interaction with leukotriene A4, with a ΔG value of -6.63 kcal/mol (Wathon et al. 2024). The D7 protein from *Ae. aegypti* forms moderately stable bonds and interactions with epinephrine, with a ΔG value of -5.8 kcal/mol. The D7 protein from *Culex quinquefasciatus* demonstrates more stable binding affinity and interaction to the hexadecanolide, as evidenced by a ΔG value of -7.82 kcal/mol (Govindan et al. 2020). Meanwhile, the D7 protein from *Anopheles gambiae* shows significantly higher and more stable binding affinity toward tryptamine (ΔG -10.1 kcal/mol) and serotonin (ΔG -11.9 kcal/mol) (Mans et al. 2007). These studies

indicate that the D7 protein from different species exhibits varying binding affinities and interactions with different ligands. This variation is likely due to the formation of different bonds between the D7 protein and diverse ligands, resulting in varying ΔG values. The variety of amino acid residues in the binding pocket of the D7 protein that interact with the ligand's atoms also plays a role in determining the type of bonds and the stability of the interactions. The spontaneous and stable binding between the 3D structure of D7 protein and TxA2 ligand indicates the potential of D7 protein in preventing platelet aggregation. This potential indicates that D7 protein from *Ae. albopictus* salivary glands can be developed as a new antiplatelet agent.

The interaction between the D7 protein and the TxA2 ligand was determined through visualizing molecular docking. The visualization helps to identify the amino acid residues of a protein that establish the stability of interaction with ligands (Furmanová et al. 2019). Various amino acid residues present in the active site help sustain interactions with ligands (Sari et al. 2020). The chemical bonds formed through interactions between the amino acids and the atoms of the test ligand can vary, such as hydrogen bonds, alkyl interactions, pi-alkyl interactions, pi-sigma interactions, and T-shaped pi-pi interactions (Kumar et al. 2021). The visualization of molecular docking results of D7 protein and TxA2 ligand is shown in Figure 6.

Table 5. The amino acid residues of D7 protein interacting with TxA2 ligand

Amino Acid Residues D7 Protein	Ligand Atoms TxA2	Chemical Bonds
Threonine 190 (THR 190)	H (Hydrogen)	Hydrogen bonds conventional
Glutamic Acid 268 (GLU 268)		
Tyrosine 178 (TYR 178)	C (Carbon)	Carbon-hydrogen bonds
Phenylalanine 154 (PHE 154)		
Isoleucine 175 (ILE 175)	-	Alkyl
Arginine 176 (ARG176)	-	
Valine 293 (VAL 293)	-	
Tyrosine 248 (TYR 248)	-	Pi-Alkyl
Tyrosine 178 (TYR 178)	-	

Table 5 shows the amino acid residues of the D7 protein interacting with TxA2 ligand. This indicates that the active site of the D7 protein can bind to the TxA2 ligand. The active sites in the D7 protein binding to TxA2 ligand are THR 190, GLU 268, TYR 178, PHE 154, ILE 175, ARG176, VAL 293, TYR 248, and TYR 178. The chemical bonds from these interactions involve hydrogen bonds conventional, carbon-hydrogen bonds, alkyl interactions, and Pi-Alkyl interactions. Conventional hydrogen bonds are formed on 2 amino acid residues, namely THR 190 and GLU 268. Carbon hydrogen bonds are formed on another pair of amino acids, TYR 178 and PHE 154. Alkyl interactions comprise 3 amino acids, namely ILE 175, ARG176, and VAL 293. Finally, Pi- Alkyl is formed in 2 amino acids, namely TYR 248 and TYR 178.

The hydrogen bond between proteins and ligands aids in binding to the active site (Kataria and Khatkar 2019). This bond occurs between hydrogen atoms and electronegative atoms, such as flour (F), nitrogen (N), or oxygen (O) (Głowacki et al. 2013). The bonds consist of conventional hydrogen bonds and carbon-hydrogen bonds. Conventional hydrogen bonds occur because the donor and acceptor atoms have strong electronegativity (Mishra et al. 2021). Carbon-hydrogen bonds occur when the donor atom is polarized carbon. A carbon-hydrogen bond is one of the weakest bonds among other hydrogen bonds (Gómez-Jeria et al. 2020). Hydrogen bonds influence the stability of protein structures because proteins are formed from NH and OH groups which act as electron donors in the formation of hydrogen bonds. As a corollary, the electrons will be received by other

groups to form chemical bonds (Dhorajiwala et al. 2019).

Alkyl interactions or bonds occur in alkyl groups, defined as a non-pi and non-polarized system in which most of the side chains are aliphatic amino acids. These amino acids include alanine, valine, leucine, isoleucine, methionine, selenomethionine, cysteine, proline, CB, CG, CD atoms of lysine, and CB and CG atoms of arginine. Alkyl is an organic chemical functional group that only contains carbon and hydrogen atoms, in the form of a chain. Pi-alkyl interactions occur in the pi electron cloud with an aromatic group and electron groups from several alkyl groups. Pi-alkyl interactions occur when the centroid of the pi ring and the alkyl group are present inside the alkyl centroid which possesses at least one pair of atoms with common pi-pi atoms (Gómez-Jeria et al. 2020).

This study involves modeling the interaction between the D7 protein from *Ae. albopictus* salivary glands and the eicosanoid molecule TxA2 as a ligand. The results of this in-silico interaction modeling provide a basic information for further analysis of D7 protein activity through in-vitro and in-vivo studies. This is crucial for understanding the role of the D7 protein in inhibiting platelet aggregation, whether by studying biological, chemical, or physical processes in a controlled environment (outside of a living organism) or by investigating biological pathways within a living organism. This approach aims to better define the potential of the D7 protein from *Ae. albopictus* as a novel antiplatelet agent.

CONCLUSION

The results of molecular docking between D7 protein from *Ae. albopictus* and TxA2 ligand shows a binding energy value of -5.60 kcal/mol. This explains that the D7 protein can bind to TxA2 molecule stably and spontaneously. The amino acid residues in the active site of the D7 protein that interact with the atoms in TxA2 ligand include THR 190, GLU 268, TYR 178, PHE 154, ILE 175, ARG176, VAL 293, TYR 248, and TYR 178. The interactions between the amino acid residues of D7 protein and TxA2 ligands generate carbon-hydrogen bonds, alkyl interactions, and Pi-Alkyl interactions. The stable and spontaneous binding mode of a protein to a ligand is a key factor in determining its potential as a candidate for biological drug development. Further exploration of the potential of the D7 protein from the salivary glands of *Ae. albopictus* through in-vitro and in-vivo analysis is crucial to specifying the target for the development of a new antiplatelet agent. This is important to study the pharmacology, pharmacokinetics, and bioavailability of the D7 protein as a biological drug. The findings have acknowledged the potential of the D7 protein from *Ae. albopictus* as a new antiplatelet agent for the development in the health and pharmaceutical sectors.

ACKNOWLEDGMENTS

This research has been financially supported by “Hibah Penelitian Dosen Pemula 2023, No. 3426/UN25.3.1/LT/2023”, LP2M – University of Jember.

REFERENCES

Afriza D, Suriyah WH, Ichwan SJA (2018) In silico analysis of molecular interactions between the anti-apoptotic protein survivin and dentatin, nordentatin, and quercetin. J Phys: Conf Ser 1073:032001. https://doi.org/10.1088/1742-6596/1073/3/032001

Ahmed MZS (2021) Homology Modeling and Structural Analysis of theFlavanone 3- Hydroxylase (F3H) and Flavonoid 3`hydroxylase (F3`H) Genes from Ginkgo biloba (L.). IOSR-JBB 7:01–21. https://doi.org/10.9790/264X-0701020121

Alhazmi MI (2015) Molecular docking of selected phytocompounds with H1N1 Proteins. Bioinformation 11:196–202. https://doi.org/10.6026/97320630011196

Alsafi MA, Hughes DL, Said MA (2020) First COVID-19 mol-ecular docking with a chalcone-based compound: synthesis, single-crystal structure and Hirshfeld surface analysis study. Acta Cryst C 76:1043–1050.

https://doi.org/10.1107/S2053229620014217

Alvarenga PH, Andersen JF (2023) An Overview of D7 Protein Structure and Physiological Roles in Blood-Feeding Nematocera. Biology 12:39. https://doi.org/10.3390/biology12010039

Alvarenga PH, Dias DR, Xu X, Francischetti IMB, Gittis AG, Arp G, Garboczi DN, Ribeiro JMC, Andersen JF (2022) Functional aspects of evolution in a cluster of salivary protein genes from mosquitoes. Insect Biochem Mol Biol 146:103785. https://doi.org/10.1016/j.ibmb.2022.103785

Arwansyah A, Ambarsari L, Sumaryada T (2014) Simulasi Docking Senyawa Kurkumin dan Analognya Sebagai Inhibitor Reseptor Androgen pada Kanker Prostat. CB 1:11–19. https://doi.org/10.29244/cb.1.1.11-19

Attique SA, Hassan M, Usman M, Atif RM, Mahboob S, Al-Ghanim KA, Bilal M, Nawaz MZ (2019) A Molecular Docking Approach to Evaluate the Pharmacological Properties of Natural and Synthetic Treatment Candidates for Use against Hypertension. Int J Environ Res Public Health 16:923. https://doi.org/10.3390/ijerph16060923

Biasini M, Bienert S, Waterhouse A, Arnold K, Studer G, Schmidt T, Kiefer F, Cassarino TG, Bertoni M, Bordoli L, Schwede T (2014) SWISS-MODEL: modelling protein tertiary and quaternary structure using evolutionary information. Nucleic Acids Res 42:W252–W258. https://doi.org/10.1093/nar/gku340

Bienert S, Waterhouse A, de Beer TAP, Tauriello G, Studer G, Bordoli L, Schwede T (2017) The SWISS-MODEL Repository—new features and functionality. Nucleic Acids Res 45:D313–D319. https://doi.org/10.1093/nar/gkw1132

Chen VB, Arendall WB, Headd JJ, Keedy DA, Immormino RM, Kapral GJ, Murray LW, Richardson JS, Richardson DC (2010) MolProbity: all-atom structure validation for macromolecular crystallography. Acta Crystallogr D Biol Crystallogr 66:12–21. https://doi.org/10.1107/S0907444909042073

Chowdhury A, Modahl CM, Missé D, Kini RM, Pompon J (2021) High resolution proteomics of Aedes aegypti salivary glands infected with either dengue, Zika or chikungunya viruses identify new virus specific and broad antiviral factors. Sci Rep 11:23696. https://doi.org/10.1038/s41598-021-03211-0

Clinton JLS, Vogt MB, Kneubehl AR, Hibl BM, Paust S, Rico-Hesse R (2023) Sialokinin in mosquito saliva shifts human immune responses towards intracellular pathogens. PLOS Neglected Tropical Diseases 17:e0011095. https://doi.org/10.1371/journal.pntd.0011095

Conway MJ, Londono-Renteria B, Troupin A, Watson AM, Klimstra WB, Fikrig E, Colpitts TM (2016) Aedes aegypti D7 Saliva Protein Inhibits Dengue Virus Infection. PLoS Negl Trop Dis 10:e0004941. https://doi.org/10.1371/journal.pntd.0004941

Dhorajiwala TM, Halder ST, Samant L (2019) Comparative In Silico Molecular Docking Analysis of L-Threonine-3-Dehydrogenase, a Protein Target Against African Trypanosomiasis Using Selected Phytochemicals. J Appl Biotechnol Rep 6:101–108. https://doi.org/10.29252/JABR.06.03.04

Duan G, Ji C, H. Zhang JZ (2020) Developing an effective polarizable bond method for small molecules with application to optimized molecular docking. RSC Adv 10:15530–15540. https://doi.org/10.1039/D0RA01483D

Endriyatno NC, Walid M (2022) Studi In Silico Kandungan Senyawa Daun Srikaya (Annona squamosa L.)Terhadap Protein Dihydrofolate Reductase Pada Mycobacterium tuberculosis. Pharmacon 19:87–98. https://doi.org/10.23917/pharmacon.v19i1.18044

Fadlan A, Nusantoro YR (2021) The Effect of Energy Minimization on The Molecular Docking of Acetone-Based Oxindole Derivatives. JKPK 6:69–77. https://doi.org/10.20961/jkpk.v6i1.45467

Ferencz L, Lucia M (2015) Identification of new superwarfarin-type rodenticides by structural similarity. The docking of ligands on the vitamin K epoxide reductase enzyme's active site. Acta Univ Sapientiae Agric Environ 7. https://doi.org/10.1515/ausae-2015-0010

Ferreira-de-Lima VH, Andrade P dos S, Thomazelli LM, Marrelli MT, Urbinatti PR, Almeida RMM de S, Lima-Camara TN (2020) Silent circulation of dengue virus in Aedes albopictus (Diptera: Culicidae) resulting from natural vertical transmission. Sci Rep 10:3855. https://doi.org/10.1038/s41598-020-60870-1

Fontaine A, Diouf I, Bakkali N, Missé D, Pagès F, Fusai T, Rogier C, Almeras L (2011) Implication of haematophagous arthropod salivary proteins in host-vector interactions. Parasites Vectors 4:187. https://doi.org/10.1186/1756-3305-4-187

Forouzesh N, Mishra N (2021) An Effective MM/GBSA Protocol for Absolute Binding Free Energy Calculations: A Case Study on SARS-CoV-2 Spike Protein and the Human ACE2 Receptor. Molecules 26:2383. https://doi.org/10.3390/molecules26082383

Furmanová K, Kozlíková B, Vonásek V, Byška J (2019) DockVis: Visual Analysis of Molecular Docking Data. EG VCBM 10 pages. https://doi.org/10.2312/VCBM.20191238

Głowacki ED, Irimia-Vladu M, Bauer S, Serdar Sariciftci N (2013) Hydrogen-bonds in molecular solids – from biological systems to organic electronics. J Mater Chem B 1:3742–3753. https://doi.org/10.1039/C3TB20193G

Gómez-Jeria J-S, Robles-Navarro A, Kpotin G, Garrido-Sáez N, Nelson G-D (2020) Some remarks about the relationships between the common skeleton concept within the Klopman-Peradejordi-Gómez QSAR method and the weak molecule-site interactions

Govindan L, Anbazhagan S, Altemimi AB, Lakshminarayanan K, Kuppan S, Pratap-Singh A, Kandasamy M (2020) Efficacy of Antimicrobial and Larvicidal Activities of Green Synthesized Silver Nanoparticles Using Leaf Extract of Plumbago auriculata Lam. Plants 9:1577. https://doi.org/10.3390/plants9111577

Guerrero D, Cantaert T, Missé D (2020) Aedes Mosquito Salivary Components and Their Effect on the Immune Response to Arboviruses. Front Cell Infect Microbiol 10

Huey WR, Morris GM, Forli S (2012) Using AutoDock 4 and AutoDock Vina with AutoDockTools: A Tutorial. The Scripps Research Institute Molecular Graphics Laboratory

Jablonka W, Kim IH, Alvarenga PH, Valenzuela JG, Ribeiro JMC, Andersen JF (2019) Functional and structural similarities of D7 proteins in the independently-evolved salivary secretions of sand flies and mosquitoes. Sci Rep 9:5340. https://doi.org/10.1038/s41598-019-41848-0

Kanduc D (2012) Homology, similarity, and identity in peptide epitope immunodefinition. J Pept Sci 18:487–494. https://doi.org/10.1002/psc.2419

Kataria R, Khatkar A (2019) In-silico design, synthesis, ADMET studies and biological evaluation of novel derivatives of Chlorogenic acid against Urease protein and H. Pylori bacterium. BMC Chemi 13:41. https://doi.org/10.1186/s13065-019-0556-0

Khor BY, Tye GJ, Lim TS, Choong YS (2015) General overview on structure prediction of twilight-zone proteins. Theor Biol Med Model 12:15. https://doi.org/10.1186/s12976-015-0014-1

Kolina J, Sumiwi S, Levita J (2019) MODE IKATAN METABOLIT SEKUNDER DI TANAMAN AKAR KUNING (Arcangelisia flava L.) DENGAN NITRAT OKSIDA SINTASE. FITOFARMAKA 8:45–52. https://doi.org/10.33751/jf.v8i1.1171

Kumar D, Kumar R, Ramajayam R, Lee KW, Shin D-S (2021) Synthesis, Antioxidant and Molecular Docking Studies of (-)-Catechin Derivatives. J Korean Chem Soc 65:106–112. https://doi.org/10.5012/jkcs.2021.65.2.106

Li Z, Ji C, Cheng J, Åbrink M, Shen T, Kuang X, Shang Z, Wu J (2022) Aedes albopictus salivary proteins adenosine deaminase and 34k2 interact with human mast cell specific proteases tryptase and chymase. Bioengineered 13:13752–13766. https://doi.org/10.1080/21655979.2022.2081652

Mans BJ, Calvo E, Ribeiro JMC, Andersen JF (2007) The Crystal Structure of D7r4, a Salivary Biogenic Amine-binding Protein from the Malaria Mosquito Anopheles gambiae*. J Biol Chem 282:36626–36633. https://doi.org/10.1074/jbc.M706410200

Marín-López A, Raduwan H, Chen T-Y, Utrilla-Trigo S, Wolfhard DP, Fikrig E (2023) Mosquito Salivary Proteins and Arbovirus Infection: From Viral Enhancers to Potential Targets for Vaccines. Pathogens 12:371. https://doi.org/10.3390/pathogens12030371

Martínez L (2015) Automatic Identification of Mobile and Rigid Substructures in Molecular Dynamics Simulations and Fractional Structural Fluctuation Analysis. PLOS ONE 10:e0119264. https://doi.org/10.1371/journal.pone.0119264

Martin-Martin I, Kern O, Brooks S, Smith LB, Valenzuela-Leon PC, Bonilla B, Ackerman H, Calvo E (2021) Biochemical characterization of AeD7L2 and its physiological relevance in blood feeding in the dengue mosquito vector, Aedes aegypti. FEBS J 288:2014–2029. https://doi.org/10.1111/febs.15524

Martin-Martin I, Smith LB, Chagas AC, Sá-Nunes A, Shrivastava G, Valenzuela-Leon PC, Calvo E (2020) Aedes albopictus D7 Salivary Protein Prevents Host Hemostasis and Inflammation. Biomolecules 10:1372. https://doi.org/10.3390/biom10101372

Minovski DN (2021) MOLECULAR DOCKING CALCULATIONS UTILIZING DISCOVERY STUDIO & PIPELINE PILOT

Mishra KK, Borish K, Singh G, Panwaria P, Metya S, Madhusudhan MS, Das A (2021) Observation of an Unusually Large IR Red-Shift in an Unconventional S–H···S Hydrogen-Bond. J Phys Chem Lett 12:1228–1235. https://doi.org/10.1021/acs.jpclett.0c03183

Oktarianti R, Khasanah RN, Wathon S, Senjarini K (2021) Detection of immunogenic protein from salivary gland of Aedes albopictus. Univ Med 40:234–242. https://doi.org/10.18051/UnivMed.2021.v40.234-242

Pratama MRF (2016) Studi Docking Molekular Senyawa Turunan Kuinolin Terhadap Reseptor Estrogen-A: Study of Molecular Docking of Quinoline Derivative Compounds against Estrogen-A Receptors. J Surya Medika 2:1–7. https://doi.org/10.33084/jsm.v2i1.215

Ramírez D, Caballero J (2018) Is It Reliable to Take the Molecular Docking Top Scoring Position as the Best Solution without Considering Available Structural Data? Molecules 23:1038. https://doi.org/10.3390/molecules23051038

Rucker D, Dhamoon AS (2024) Physiology, Thromboxane A2. In: StatPearls. StatPearls Publishing, Treasure Island (FL)

Saputra DPD, Susanti NMP (2018) Molecular Docking Sianidin dan Peonidin sebagai Antiinflamasi pada Aterosklerosis secara In Silico. JFU 7:28–33

Sari IW, Junaidin J, Pratiwi D (2020) STUDI MOLECULAR DOCKING SENYAWA FLAVONOID HERBA KUMIS KUCING (Orthosiphon stamineus B.) PADA RESEPTOR α-GLUKOSIDASE

SEBAGAI ANTIDIABETES TIPE 2. FARM 7:54. https://doi.org/10.47653/farm.v7i2.194

Sastry GM, Adzhigirey M, Day T, Annabhimoju R, Sherman W (2013) Protein and ligand preparation: parameters, protocols, and influence on virtual screening enrichments. J Comput Aided Mol Des 27:221–234. https://doi.org/10.1007/s10822-013-9644-8

Sharma S, Sarkar S, Paul SS, Roy S, Chattopadhyay K (2013) A small molecule chemical chaperone optimizes its unfolded state contraction and denaturant like properties. Sci Rep 3:3525. https://doi.org/10.1038/srep03525

Shrivastava G, Valenzuela-Leon PC, Chagas AC, Kern O, Botello K, Zhang Y, Martin-Martin I, Oliveira MB, Tirloni L, Calvo E (2022) Alboserpin, the Main Salivary Anticoagulant from the Disease Vector Aedes albopictus, Displays Anti–FXa-PAR Signaling In Vitro and In Vivo. ImmunoHorizons 6:373–383. https://doi.org/10.4049/immunohorizons.2200045

Studer G, Rempfer C, Waterhouse AM, Gumienny R, Haas J, Schwede T (2020) QMEANDisCo—distance constraints applied on model quality estimation. Bioinformatics 36:1765–1771. https://doi.org/10.1093/bioinformatics/btz828

Susanti NMP, Laksmiani NPL, Noviyanti NKM, Arianti KM, Duantara IK (2019) MOLECULAR DOCKING TERPINEN-4-OL SEBAGAI ANTIINFLAMASI PADA ATEROSKLEROSIS SECARA IN SILICO. JCHEM 221. https://doi.org/10.24843/JCHEM.2019.v13.i02.p16

Szczuko M, Kozioł I, Kotlęga D, Brodowski J, Drozd A (2021) The Role of Thromboxane in the Course and Treatment of Ischemic Stroke: Review. Int J Mol Sci 22:11644. https://doi.org/10.3390/ijms222111644

Torres PHM, Sodero ACR, Jofily P, Silva-Jr FP (2019) Key Topics in Molecular Docking for Drug Design. Int J Mol Sci 20:4574. https://doi.org/10.3390/ijms20184574

Umamaheswari M, Madeswaran A, Asokkumar K (2013) Virtual Screening Analysis and In-vitro Xanthine Oxidase Inhibitory Activity of Some Commercially Available Flavonoids. Iran J Pharm Res 12:317–323

Wang C, Cao X, Dong M, Zhang L, Liu J, Cao X, Xue X (2021) Theoretical Calculation of Self-Propagating High-Temperature Synthesis (SHS) Preparation of AlB12

Wathon S, Afkarina I, Rohmah U, Oktarianti R, Senjarini K (2022a) In Vitro Analysis of Human IgG Immune Response Against 31 kDa and 67 kDa Immunogenic Protein from Aedes albopictus Salivary Glands. In 4th International Conference on Life Sciences and Biotechnology (ICOLIB 2021) 122–134

Wathon S, Oktarianti R, Senjarini K (2024) Molecular Docking of Interaction between D7 Protein from the Salivary Gland of *Aedes aegypti* and Leukotriene A_4 for Developing Thrombolytic Agent. BIO Web Conf 101:04002. https://doi.org/10.1051/bioconf/202410104002

Wathon S, Purwati W, Oktarianti R, Senjarini K (2022b) IgG IMMUNE RESPONSE AGAINST SALIVARY GLAND PROTEIN EXTRACT OF DENGUE VECTOR Aedes aegypti. J Appl Biol Sci 16:483–492

Wichit S, Ferraris P, Choumet V, Missé D (2016) The effects of mosquito saliva on dengue virus infectivity in humans. Curr Opin Virol 21:139–145. https://doi.org/10.1016/j.coviro.2016.10.001

Xiang Q, Pang X, Liu Z, Yang G, Tao W, Pei Q, Cui Y (2019) Progress in the development of antiplatelet agents: Focus on the targeted molecular pathway from bench to clinic. Pharmacol Therapeut 203:107393. https://doi.org/10.1016/j.pharmthera.2019.107393